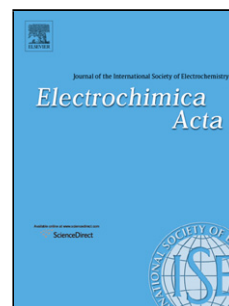


Accepted Manuscript

Title: Protic plastic crystal/PVDF composite membranes for Proton Exchange Membrane Fuel Cells under non-humidified conditions

Authors: M. Díaz, A. Ortiz, J.M. Pringle, X. Wang, R. Vijayaraghavan, D.R. MacFarlane, M. Forsyth, I. Ortiz



PII: S0013-4686(17)31493-7
DOI: <http://dx.doi.org/doi:10.1016/j.electacta.2017.07.076>
Reference: EA 29893

To appear in: *Electrochimica Acta*

Received date: 21-4-2017
Revised date: 24-6-2017
Accepted date: 12-7-2017

Please cite this article as: M.Díaz, A.Ortiz, J.M.Pringle, X.Wang, R.Vijayaraghavan, D.R.MacFarlane, M.Forsyth, I.Ortiz, Protic plastic crystal/PVDF composite membranes for Proton Exchange Membrane Fuel Cells under non-humidified conditions, *Electrochimica Acta* <http://dx.doi.org/10.1016/j.electacta.2017.07.076>

This is a PDF file of an unedited manuscript that has been accepted for publication. As a service to our customers we are providing this early version of the manuscript. The manuscript will undergo copyediting, typesetting, and review of the resulting proof before it is published in its final form. Please note that during the production process errors may be discovered which could affect the content, and all legal disclaimers that apply to the journal pertain.

**Protic plastic crystal/PVDF composite membranes for Proton Exchange
Membrane Fuel Cells under non-humidified conditions**

M. Díaz^a, A. Ortiz^a, J. M. Pringle^b, X. Wang^b, R. Vijayaraghavan^c, D. R. MacFarlane^c, M. Forsyth^b, I. Ortiz^{a,*}

^aChemical and Biomolecular Engineering Department. University of Cantabria.
Avenida de los Castros s/n 39005, Santander (Spain)

^bDeakin University, Geelong, Australia, ARC Centre of Excellence for
Electromaterials Science, Institute for Frontier Materials.

^cSchool of Chemistry, Monash University, Clayton, VIC 3800, Australia

*Corresponding author. E-mail address: ortizi@unican.es

Abstract

Composite membranes based on the protic plastic crystal *N,N*-dimethylethylenediammonium triflate [DMEDAH][TFO] and poly(vinylidene fluoride) (PVDF) nanofibers have been developed for proton exchange membrane fuel cells (PEMFCs) under non-humidified conditions. The effect of addition of 5 mol% triflic acid or 5 mol% of the base *N,N*-dimethylethylenediamine on the thermal and transport properties of the material is discussed. The acid-

doped plastic crystal reports more than double the ionic conductivity of the pure plastic crystal. The effects of doping the plastic crystal and the composites, with acid or base, on the ionic conductivity and fuel cell performance are reported. Composite membranes based on PVDF nanofibers and [DMEDAH][TFO] were tested in a single PEMFC. The results show the potential of these composite membranes to be used as electrolytes in this electrochemical application without external humidification.

1. Introduction

The unique properties of organic ionic plastic crystals (OIPCs) make them promising solid electrolytes for fuel cell applications. Their negligible volatility and high thermal and electrochemical stability make them suitable for electrochemical devices [1-3]. These materials have the advantages of protic ionic liquids (i.e. high proton conductivity without humidification) plus the benefits of a solid state electrolyte [4,5]. OIPCs are usually formed by a large symmetric organic cation and an inorganic anion that is normally symmetrical or has a delocalised charge. These materials typically undergo one or more solid-solid phase transition before melting, which are associated to the beginning of rotational or translational motions of the ions. This leads to progressive transformation from an ordered crystalline phase to an increasingly disordered structure. The highest temperature solid phase is denoted phase I; the lower temperature phases are phases II, III, and so forth [6]. The conductivity of these materials is attributed to the presence of defects or vacancies in the crystalline structure, the rotational and translational disorder of the cation and anion, and the conformational disorder of the ions [7]. They are referred to as “plastic crystals” due to their

softness; they are easily deformed under stress. This deformation occurs due to the mobility of the slip planes, and dislocation or vacancy migration. The malleability should be beneficial for use of the material in fuel cell devices as it will afford better contact with the electrodes and increased tolerance of this contact to any volume changes [8]. For electrochemical applications, plastic crystals are often used as matrix materials for added dopant ions, e.g. target ion such as Li^+ for lithium batteries or I^-/I_3^- for dye-sensitized solar cells. This doping can also significantly increase the ionic conductivity [9-12].

Among the different types of OIPCs, protic plastic crystals are being studied as promising electrolytes for fuel cells. These compounds can be easily obtained by combining a Brønsted acid and a Brønsted base. As for protic ionic liquids, protic plastic crystals are formed by transfer of protons from the acid to the base, leading to the presence of proton donor and acceptor sites that can be used to build a hydrogen-bonded network [13]. In the early work by Yoshizawa-Fujita *et al.* [14] choline dihydrogen phosphate [choline][DHP] and 1-butyl-3-methylimidazolium dihydrogen phosphate [C_4mim][DHP] were synthesized as new proton-conducting ionic plastic crystals. [C_4mim][DHP] showed a solid-solid phase transition and a melting point at 23 and 119 °C, respectively, whereas [choline][DHP] displayed solid-solid phase transitions at 45 and 71 °C and melting point at 167 °C. Ionic conductivities ranged from $1.0 \times 10^{-6} \text{ S.cm}^{-1}$ at room temperature to $1.0 \times 10^{-3} \text{ S.cm}^{-1}$ in the plastic crystalline phase for choline dihydrogen phosphate, and up to $1.0 \times 10^{-5} \text{ S.cm}^{-1}$ at 90 °C for 1-butyl-3-methylimidazolium dihydrogen phosphate. The [choline][DHP] showed one order of magnitude higher ionic conductivity than [C_4mim][DHP] in phase I, revealing that the hydroxyl group might be involved in fast proton transport in the solid state.

The proton conduction in choline dihydrogenphosphate [choline][DHP] has been well studied, initially prompted by the excellent proton conductivities of phosphoric-acid-based materials. The proton transport of this material is proposed to be facilitated by a three-fold rotation of the dihydrogenphosphate anion [15,16]. High proton diffusivities can be obtained after doping with acid [17]. The thermal stability of [choline][DHP] doped with phosphoric acid is good, with minimal weight loss up to 200 °C. However, this OIPC with 18 mol% added phosphoric acid presents an amorphous phase. In contrast, using 4 wt% triflic acid or bis(trifluoromethanesulfonyl)amide (Tf₂N) acid improves the conductivity while still maintaining the solid state. Moreover, [choline][DHP] doped with 4 mol% triflic acid achieved significant proton reduction currents in the cyclic voltammetry, which is an important indicator of potential fuel cell performance [16,18].

The proton transport behavior in guanidinium triflate (GTf) solid and its mixtures with triflic acid has been studied by Zhu and co-workers [19]. Both the pure GTf and 1 mol% acid doped samples showed relatively low conductivity and strong temperature dependence. Nevertheless, for the samples containing 2 mol% acid or more, the conductivities are high ($1.0 \times 10^{-3} \text{ S.cm}^{-1}$) and relatively independent of temperature. For all the measured temperatures, an increase in the conductivity compared to the pure material was observed for acid contents of 1 and 2 mol%. This behavior was considered to be a strong indication of percolation-dominated conducting mechanisms within the system. However, at high temperatures the GTf matrix also becomes conductive and contributes to the conductivity of the composites. A guanidinium-based protic plastic crystal was also studied by Chen *et al.* [20]. In that work, guanidinium nonaflate was reported

as a new plastic crystal with significant ionic conductivity in phase I (1.0×10^{-4} S.cm⁻¹ at 176 °C) and high thermal stability (408 °C).

In the work reported by Luo *et al.* [21], 1,2,4-triazolium perfluorobutanesulfonate was considered as anhydrous proton conductor for high temperature fuel cells. The ionic conductivity dependence with temperature was correlated with the phase transitions observed in the material, reaching 1.27×10^{-6} S.cm⁻¹ in phase I (155 °C). During fuel cell testing at 150 °C without humidity, open circuit voltage (OCV) of 1.05 V and a current density around 17 μ A.cm⁻² at 0.2 V were obtained. To improve the mechanical stability of the electrolytes, OIPCs can be combined with a commercial polymer that acts as a support [22-25]. Thus, proton conducting membranes based on impregnated cellulose acetate supports with mixtures of choline dihydrogen phosphate and various acids were synthesized by Rana *et al.* for fuel cell applications [17]. A membrane doped with 4 mol% HNTf₂ containing up to 50 wt% water showed an OCV of approximately 0.78 V at 125 °C.

Composite membranes of electrospun PVDF nanofibers and OIPC have recently been shown to perform well as solid-state electrolytes in batteries. For example, with the plastic crystal *N*-methyl-*N*-ethylpyrrolidinium tetrafluoroborate [C₂mpyr][BF₄], OIPC/PVDF nanofiber composites can exhibit enhanced conductivity compared to that of the bulk plastic crystal, plus excellent thermal, mechanical and electrochemical stability. [26] Composite nanofibers based on the same plastic crystal and polymer can also be prepared by co-electrospinning, and the increased ionic conductivity of these composites is beneficial for their use as solid-state electrolytes for batteries [27].

Driven by the advantages of protic plastic crystals and electrospun nanofibers, here we report the development of composite membranes based on the protic plastic crystal *N,N*-dimethylethylene diammonium triflate [DMEDAH][TFO], [28] combined with poly(vinylidene fluoride) (PVDF) electrospun nanofibers, for use in PEMFCs under non-humidified conditions. The effect of the addition of 5 mol% of triflic acid or 5 mol% of *N,N*-dimethylethylenediamine to the pure plastic crystal and to [DMEDAH][TFO]/PVDF composite membranes on the ionic conductivity and thermal behavior is discussed. Furthermore, the fuel cell performance of the synthesized composite membranes based on PVDF nanofibers and pure and doped [DMEDAH][TFO] membranes was also tested.

2. Experimental methods

2.1. Materials

PVDF powder (MW 534000), *N,N*-dimethylethylenediamine (99.5%) and triflic acid (98%) were purchased from Sigma-Aldrich and used as received.

2.2. Fabrication of composite membranes

2.2.1. Synthesis of [DMEDAH][TFO]

N,N-dimethylethylenediammonium triflate, [DMEDAH][TfO], was made and analysed as reported previously [28] by the proton transfer reaction between triflic acid and *N,N*-dimethylethylenediamine. The synthesis was performed by drop-wise addition of aqueous solution of triflic acid (42 mmoles) to *N,N*-dimethylethylenediamine (42 mmoles) in an ice bath, and the reactants were then stirred for 2 hours at room temperature. The water was then removed by

distillation and the final solid product was dried under vacuum at 70 °C for two days. The yield was 98 %. The stoichiometry of the acid–base reaction was verified by an aqueous titration method and the OIPC samples were tested for correct pH after dilution into water (0.1 M). This is a sensitive, routine test of the final stoichiometry for these materials. The pH of 0.1 M aqueous solution was 8.0. Electro spray mass spectroscopy analysis, (cone $\pm 25V$): [DMEDAH][TfO], m/z (relative intensity, %): ES⁺, 89.2 ($(CH_3)_2N^+CH_2CH_2NH_3$ 100); ES⁻, 149.0 ($CF_3SO_3^-$, 100).

The 5 mol % triflic acid doped sample was made by adding an aqueous solution containing 2.26 g (95 mol %) of [DMEDAH][TfO] to another aqueous solution containing 0.075 g (5 mol%) of triflic acid. The reactants were stirred to obtain a clear liquid and then distilled under reduced pressure at 70 °C to remove the water. The solid was dried under vacuum at room temperature and the yield was 98 %. The pH of 0.1 M aqueous solution was 7.4.

The 5 mol % *N,N*-dimethylethylenediamine doped sample was synthesized by adding an aqueous solution of 2.26 g (95 mol%) of [DMEDAH][TfO] to an aqueous solution of 0.04 g (5 mol%) *N,N*-dimethylethylenediamine. The reactants were stirred and then distilled under reduced pressure at 70 °C to remove the water. The solid was dried under vacuum at room temperature and the yield was 98 %. The pH of a 0.1 M aqueous solution was 7.9.

2.2.2. Electrospinning of nanofibers

1.5 g PVDF was dissolved in a mixture of 3 ml of DMF and 7 ml of acetone and heated at 60 °C for 30 min until the solution was homogeneous. The solution was transferred into a plastic syringe and discharged at 1 ml.h⁻¹ using a syringe pump (KD Scientific) into a 15 kV electric field between the syringe needle (21G) and a

grounded metal collector (distance 15 cm). The fibers were accumulated randomly on the collector.

2.2.3. Fabrication of composite membranes

The [DMEDAH][TFO] and nanofibers were dried overnight at 40 °C on a vacuum line. Composite membranes were synthesised by a melt casting technique. The plastic crystal (90 wt%) was spread on the nanofiber surface (10 wt%) and melted at 70 °C on a hot plate. Composite membranes were kept in a vacuum oven at 80 °C overnight to completely melt the plastic crystal and to remove any residual traces of water before fuel cell measurement. Then, the membrane was pressed to ensure homogeneous distribution of the plastic crystal between the fibers. Fuel cell testing and ionic conductivity measurements require different sample dimensions: for ionic conductivity measurements, the membrane (10 mm diameter) was pressed between two Teflon disks in a KBr cell at 1 ton pressure, whereas for fuel cell experiments, the composite membrane (5 cm²) was pressed at 1100 psi for 3 minutes using a Carver 4386 press.

Figure 1 shows the chemical structures of [DMEDAH][TFO] and the PVDF used in this work.

2.3. Membrane characterization

2.3.1. Scanning electron microscope (SEM)

The morphology of the electrospun membranes was characterized using a JCM-5000, NeoScope, JEOL Benchtop SEM. SEM images were collected using the JCM-5000 software, with accelerating voltage of 10 kV.

2.3.2. Differential scanning calorimetry (DSC)

A Mettler Toledo DSC instrument, calibrated with cyclohexane, was used to study the thermal behavior of the materials. All samples were prepared and sealed in a glove box under argon atmosphere. Samples were scanned from -95 °C to 120 °C, at heating and cooling rates of 5 and -2 °C.min⁻¹, respectively. Two temperature scans were run; the second heating scan is reported in this work. DSC curves were normalized with respect to the pure plastic crystal weight (mW.mg⁻¹ of pure OIPC). In the traces, the peak temperatures are labeled, with an uncertainty margin of +/- 1 °C.

2.3.3. Ionic conductivity

Solid-state ionic conductivity of the materials was evaluated using electrochemical impedance spectroscopy on a Solartron potentiostat. The samples were sandwiched between pre-polished and dried circular stainless steel electrodes located inside hermetically-sealed barrel cells (Advanced Industrial Services, Moorabbin, Australia). Pellets of pure and doped plastic crystal were obtained by pressing the material at 1 ton pressure inside a KBr die (10 mm diameter). All materials were handled inside an argon glove box. A tubular Helios furnace (28 V/32 W) with a flexible ceramic heater was used to apply the temperature ramp. A Eurotherm 3504 temperature controller, interfaced to the potentiostats, allowed impedance data to be acquired automatically throughout a programmed temperature profile. A T type thermocouple with an accuracy of ± 1 °C was used for the temperature measurements. The temperature stabilization time between measurements was 30 min, and measurements were taken at 5 °C intervals. Data were collected at each temperature by applying a sinusoidal signal with amplitude of 100 mV over a frequency range of 1 MHz to 1 Hz. Conductivity values were calculated from

Nyquist plots in which the touchdown point of the semicircle corresponds to the bulk resistance of the ion-conducting media.

2.3.4. Fuel cell testing

Gas diffusion electrodes (GDEs) ($3.0 \text{ mg Pt.cm}^{-2}$, Baltic Fuel Cell GmbH) were placed at both sides of the membrane to form the membrane electrode assembly (MEA). The membrane performance was tested in a fuel cell of 5 cm^2 containing serpentine channels and equipped with a piston that ensures good contact between the internal components of the cell (quick CONNECT, Baltic Fuel Cells GmbH). The anode was fed with hydrogen at a flow rate of 50 ml.min^{-1} , while the cathode was fed with air at a rate of 100 ml.min^{-1} . The system pressure was fixed at 1.0 bar and the experiments were carried out at $25 \text{ }^\circ\text{C}$. Polarization curves of cell voltage versus electric current were obtained using an external load (ZS, H&H) under potentiostatic control at non-humidified conditions.

3. Results and discussion

3.1. Membrane synthesis

Composite membranes containing 90 wt% plastic crystal and 10 wt% nanofibers were prepared by melt casting, before being held in a vacuum oven at $80 \text{ }^\circ\text{C}$ overnight to completely melt the plastic crystal and pressed to ensure homogeneous distribution of the plastic crystal between fibers. This compositional ratio of 90/10 wt% OIPC/PVDF was selected because a lower proportion of OIPC led to composite membranes with poorly distributed OIPC within the polymeric nanofibers. SEM images of both sides of the composite membrane based on pure [DMEDAH][TFO]/PVDF (90/10 wt%) are shown in Figure 2.

These show that the OIPC completely covers the nanofibers and the voids between them, achieving a homogeneous distribution of the plastic crystal within the polymer nanofibers.

The membranes obtained were flexible and homogeneous. The average thickness was about 70 microns.

3.2. Thermal behavior

Figure 3 shows thermal traces obtained from DSC measurements of pure, 5 mol% acid-doped and 5 mol% base-doped [DMEDAH][TFO]. The OIPC shows a solid-solid phase transition at 55 °C and stays in the solid plastic phase I up to its melting temperature around 70 °C. In the acid-doped [DMEDAH][TFO], the peak corresponding to the solid-solid phase transition increased in intensity. However, when base is added to [DMEDAH][TFO], the peak is significantly decreased.

To analyze the influence of nanofibers on the thermal properties of the OIPC, DSC measurements of the PVDF composite membranes were performed (figure 4). These samples all now show one peak at around 60 °C, and a further peak at ~96 °C. From the shape of these transitions, and the thermal properties of the pure materials, these are assigned to the solid-solid phase transition and melt of the OIPC-based material respectively. This form of relatively spread-out melting transition has been observed previously in OIPCs,[6] attributed to the influence of vacancies/disorder within the structure. The peak around 96 °C was observed in both the PVDF systems and also in analogous composites with sulfonated poly(ether ether ketone) (SPEEK) fibres; this is a region in which the pure polymers have no transitions, suggesting that it represents the melting of a more highly ordered OIPC structure. This is also consistent with the observed decrease in conductivity in the composites, discussed below. In addition to this, an

exothermic peak around 25 °C is now evident in the composites, corresponding to a crystallization event. This peak, observed only during the second heating scan, indicates that the OIPC material did not fully crystallize during the cooling scan; instead, full crystallization does not occur until the heating run, when the material has enough energy to rearrange and solidify. Apart from this crystallization peak observed during the second heating scan, no other differences between the two scans were observed. The appearance of this new crystallisation peak is further evidence that the presence of PVDF fibres has a significant impact on the thermal behavior of the OIPC-based materials.

3.3. Ionic conductivity

The ionic conductivities of the materials as a function of temperature are shown in figures 5 and 6 and table 1. The conductivity of all samples increases gradually with temperature, reaching $2.7 \times 10^{-5} \text{ S.cm}^{-1}$ at 50 °C for pure [DMEDAH][TFO]. The addition of 5 mol% of triflic acid to the pure OIPC more than doubles the conductivity. This enhancement can be associated with an increase in the number of dissociable protons as a result of the acid doping [28]. Zhu *et al.* [19] showed, by ^1H NMR spectroscopy, that the fast mobility of the triflic acid protons affects the molecular dynamics of neat guanidinium triflate and its conductivity. However, when the base *N,N*-dimethylethylenediamine was added to the pure OIPC the ionic conductivity decreased especially at higher temperatures, possibly because of strong proton coupling.

Incorporation of the OIPC into the PVDF membrane decreases the conductivity, as observed previously for other types of OIPC/PVDF composites. However, both acid and base doping result in an increase in conductivity of the resulting

composite. Perhaps surprisingly, in contrast to the systems without PVDF, the highest ionic conductivity composite was for the base-doped [DMEDAH][TFO] ($4.3 \times 10^{-5} \text{ S.cm}^{-1}$ at $50 \text{ }^\circ\text{C}$, compared to $1.1 \times 10^{-5} \text{ S.cm}^{-1}$ obtained with pure [DMEDAH][TFO]). At lower temperatures, the difference in ionic conductivity is more noticeable, increasing more than one order of magnitude when 5 mol% base is added ($4.1 \times 10^{-7} \text{ S.cm}^{-1}$ to $5.7 \times 10^{-6} \text{ S.cm}^{-1}$ at $30 \text{ }^\circ\text{C}$). The addition of acid also improves the ionic conductivity, to $2.4 \times 10^{-5} \text{ S.cm}^{-1}$ at $50 \text{ }^\circ\text{C}$

3.4. Fuel cell testing

Figure 7 shows the polarization curves obtained with PVDF-based membranes containing pure [DMEDAH][TFO], 5 mol% acid-doped [DMEDAH][TFO] and 5 mol% base-doped [DMEDAH][TFO]. Pure [DMEDAH][TFO]/PVDF composite membranes gave a poor fuel cell performance, yielding an open circuit voltage (OCV) of about 0.53 V and current density of 0.45 mA.cm^{-2} at 0.15 V and $25 \text{ }^\circ\text{C}$. The addition of 5 mol% *N,N*-dimethylethylenediamine did not noticeably improve the fuel cell performance compared to that of pure [DMEDAH][TFO] conversely to what was expected after the values of ex-situ ionic conductivity. However, when 5 mol% of triflic acid was added to the plastic crystal, the performance improved significantly, reaching an OCV of 0.74 V and current density of 61 mA.cm^{-2} at 0.15 V and $25 \text{ }^\circ\text{C}$. This behavior is in accordance with the higher conductivity of the acid-doped-plastic crystal compared to pure OIPC. The high mobility of the dissociable protons from the triflic acid promotes the proton transport mechanism across the composite membrane, which enhances the fuel cell performance. In contrast, the hypothesized strong coupling of the protons in

the base-doped sample does not lead to a noteworthy increase in the fuel cell performance, despite the fact that this material has the highest total ionic conductivity, reiterating the importance of proton conduction.

To the best of our knowledge, the composite membranes developed in this work have shown highest PEMFC current density under non-humidified conditions reported thus-far for OIPC-based membranes. Prior work by Luo and coworkers [21] on high temperature fuel cells has reported an OCV of 1.05 V but a relatively low current density, of around $17 \mu\text{A}\cdot\text{cm}^{-2}$ at 0.2 V, with 1,2,4-triazolium perfluorobutanesulfonate at 150 °C without humidity. In the work of Rana *et al.* [17], proton-conducting membranes based on impregnated cellulose acetate supports with mixtures of choline dihydrogen phosphate and various acids were synthesized for fuel cell applications. The maximum load applied was 30 mA with a stable OCV of 0.11 V for the membrane doped with 4 mol% HNTf₂ at 80 °C containing up to 50 wt% water. However, that material required the presence of water to achieve these voltages.

4. Conclusions

Composite membranes based on the protic plastic crystal *N,N*-dimethylethylene diammonium triflate [DMEDAH][TFO] and poly(vinylidene fluoride) (PVDF) nanofibers have been developed for proton exchange membrane fuel cells (PEMFCs) and successfully applied under non-humidified conditions. Thermal characterization of the [DMEDAH][TFO] revealed a solid-solid phase transition at 55 °C before its melting point at 70 °C. The ionic conductivity of [DMEDAH][TFO] increased with temperature, reaching $2.7 \times 10^{-5} \text{ S}\cdot\text{cm}^{-1}$ at 50 °C.

To enhance the ionic conductivity of the plastic crystal, 5 mol% triflic acid or 5 mol% of the base *N,N*-dimethylethylenediamine were added. The conductivity of

the acid-doped plastic crystal doubled, due to the mobility of the triflic acid protons. However, the addition of the base did not enhance the ionic conductivity. Composite membranes based on PVDF and pure, acid-doped or base-doped plastic crystal were developed and characterized. In a single proton exchange membrane fuel cell (PEMFC), the membrane based on pure [DMEDAH][TfO]/PVDF showed an open circuit voltage (OCV) of about 0.53 V and a current density of 0.45 mA.cm⁻² at 0.15 V and 25 °C. The addition of 5 mol% of the base *N,N*-dimethylethylenediamine did not improve the PEMFC performance when compared to pure membranes; these results, not expected from the trend of the ex-situ ionic conductivity values, highlight the relevance of fuel cell testing of new materials. Finally, the addition of triflic acid improved the fuel cell performance, reaching an OCV of 0.74 V and current density of 61 mA.cm⁻² at 0.15 V and 25 °C. This demonstrates the potential of composite membranes based on electrospun polymers and doped protic plastic crystals to be used as proton exchange membranes for fuel cell applications without external humidification.

5. Acknowledgements

The authors acknowledge funding from the Australian Research Council (ARC) through its Centre of Excellence program, through the Australian Laureate Fellowship scheme for D.R.M and M.F, and Discovery Project DP140101535. In addition, M.D., A.O. and I.O acknowledge Spanish Ministry of Economy and Competitiveness for the project CTQ2015-66078-R (MINECO/FEDER, UE). M. D. is grateful to the Spanish Ministry of Education, Culture and Sport for the FPU2012-3721.

6. References

- [1] A. Mondal, A.P. Sunda, S. Balasubramanian, Thermal phase behavior and ion hopping in a 1,2,4-triazolium perfluorobutanesulfonate protic organic ionic plastic crystal, *Phys. Chem. Chem. Phys.* 18 (2016) 2047-2053.
- [2] K. Romanenko, L. Jin, P. Howlett, M. Forsyth, In Situ MRI of Operating Solid-State Lithium Metal Cells Based on Ionic Plastic Crystal Electrolytes, *Chem. Mater.* 28 (2016) 2844-2851.
- [3] X. Zhu, R. Zhao, W. Deng, X. Ai, H. Yang, Y. Cao, An All-solid-state and All-organic Sodium-ion Battery based on Redox-active Polymers and Plastic Crystal Electrolyte, *Electrochim. Acta* 178 (2015) 55-59.
- [4] M. Díaz, A. Ortiz, M. Isik, D. Mecerreyes, I. Ortiz, Highly conductive electrolytes based on poly([HSO₃-BVIm][TfO])/[HSO₃-BMIm][TfO] mixtures for fuel cell applications, *Int J Hydrogen Energy* 40 (2014) 11294-11302.
- [5] M. Díaz, A. Ortiz, I. Ortiz, Progress in the use of ionic liquids as electrolyte membranes in fuel cells, *J. Membr. Sci.* 469 (2014) 379-396.
- [6] J.M. Pringle, P.C. Howlett, D.R. MacFarlane, M. Forsyth, Organic ionic plastic crystals: Recent advances, *J. Mater. Chem.* 20 (2010) 2056-2062.
- [7] J.M. Pringle, Recent progress in the development and use of organic ionic plastic crystal electrolytes, *Phys. Chem. Chem. Phys.* 15 (2013) 1339-1351.

- [8] U.A. Rana, M. Forsyth, D.R. Macfarlane, J.M. Pringle, Toward protic ionic liquid and organic ionic plastic crystal electrolytes for fuel cells, *Electrochim. Acta* 84 (2012) 213-222.
- [9] K. Liu, F. Ding, Q. Lu, J. Liu, Q. Zhang, X. Liu, Q. Xu, A novel plastic crystal composite polymer electrolyte with excellent mechanical bendability and electrochemical performance for flexible lithium-ion batteries, *Solid State Ionics* 289 (2016) 1-8.
- [10] X. Li, Z. Zhang, S. Li, L. Yang, S. Hirano, Polymeric ionic liquid-plastic crystal composite electrolytes for lithium ion batteries, *J. Power Sources* 307 (2016) 678-683.
- [11] F. Chen, J.M. Pringle, M. Forsyth, Insights into the transport of alkali metal ions doped into a plastic crystal electrolyte, *Chem. Mater.* 27 (2015) 2666-2672.
- [12] N.U. Taib, N.H. Idris, Plastic crystal-solid biopolymer electrolytes for rechargeable lithium batteries, *J. Membr. Sci.* 468 (2014) 149-154.
- [13] T.L. Greaves, C.J. Drummond, Protic ionic liquids: Properties and applications, *Chem. Rev.* 108 (2008) 206-237.
- [14] M. Yoshizawa-Fujita, K. Fujita, M. Forsyth, D.R. MacFarlane, A new class of proton-conducting ionic plastic crystals based on organic cations and dihydrogen phosphate, *Electrochem. Commun.* 9 (2007) 1202-1205.
- [15] L.S. Cahill, U.A. Rana, M. Forsyth, M.E. Smith, Investigation of proton dynamics and the proton transport pathway in choline dihydrogen phosphate using solid-state NMR, *Phys. Chem. Chem. Phys.* 12 (2010) 5431-5438.

- [16] U.A. Rana, P.M. Bayley, R. Vijayaraghavan, P. Howlett, D.R. MacFarlane, M. Forsyth, Proton transport in choline dihydrogen phosphate/H₃PO₄ mixtures, *Phys. Chem. Chem. Phys.* 12 (2010) 11291-11298.
- [17] U.A. Rana, I. Shakir, R. Vijayaraghavan, D.R. MacFarlane, M. Watanabe, M. Forsyth, Proton transport in acid containing choline dihydrogen phosphate membranes for fuel cell, *Electrochim. Acta* 111 (2013) 41-48.
- [18] U.A. Rana, R. Vijayaraghavan, D.R. MacFarlane, M. Forsyth, Plastic crystal phases with high proton conductivity, *J. Mater. Chem.* 22 (2012) 2965-2975.
- [19] H. Zhu, U.A. Rana, V. Ranganathan, L. Jin, L.A. O'Dell, D.R. MacFarlane, M. Forsyth, Proton transport behaviour and molecular dynamics in the guanidinium triflate solid and its mixtures with triflic acid, *J. Mater. Chem. A* 2 (2014) 681-691.
- [20] X. Chen, H. Tang, T. Putzeys, J. Sniekers, M. Wübbenhorst, K. Binnemans, J. Fransaer, D. E. De Vos, Q. Li, J. Luo, Guanidinium nonaflate as a solid-state proton conductor, *J. Mater. Chem. A* 4 (2016) 12241-12252.
- [21] J. Luo, A.H. Jensen, N.R. Brooks, J. Sniekers, M. Knipper, D. Aili, Q. Li, B. Vanroy, M. Wübbenhorst, F. Yan, L. V. Meervelt, Z. Shao, J. Fang, Z.-H. Luo, D. E. De Vos, K. Binnemans, J. Fransaer, 1,2,4-Triazolium perfluorobutanesulfonate as an archetypal pure protic organic ionic plastic crystal electrolyte for all-solid-state fuel cells, *Energy Environ. Sci.* 8 (2015) 1276-1291.
- [22] N. Iranipour, D.J. Gunzelmann, A. Seeber, J. Vongsvivut, C. Doherty, F. Ponzio, L. A. O'Dell, A. F. Hollenkamp, M. Forsyth, P. C. Howlett, Ionic transport

through a composite structure of N-ethyl-N-methylpyrrolidinium tetrafluoroborate organic ionic plastic crystals reinforced with polymer nanofibres, *J. Mater. Chem. A* 3 (2015) 6038-6052.

[23] G.W. Greene, F. Ponzio, N. Iranipour, H. Zhu, A. Seeber, M. Forsyth, P. C. Howlett, Enhanced ionic mobility in Organic Ionic Plastic Crystal - Dendrimer solid electrolytes, *Electrochim. Acta* 175 (2015) 214-223.

[24] D. Hambali, Z. Zainuddin, I. Supa'at, Z. Osman, Studies of plastic crystal gel polymer electrolytes based on poly(vinylidene chloride-co-acrylonitrile), *AIP Conf. Proc.* 1711 (2016).

[25] M. Suleman, M. Deraman, M.A.R. Othman, R. Omar, M.A. Hashim, N.H. Basri, N. S. M. Nor, B. N. M. Dolah, M. F. Y. M. Hanappi, E. Hamdan, Electric double-layer capacitors with tea waste derived activated carbon electrodes and plastic crystal based flexible gel polymer electrolytes, *J. Phys. Conf. Ser.* 739 (2016).

[26] P.C. Howlett, F. Ponzio, J. Fang, T. Lin, L. Jin, N. Iranipour, J. Efthimiadis, Thin and flexible solid-state organic ionic plastic crystal-polymer nanofibre composite electrolytes for device applications, *Phys. Chem. Chem. Phys.* 15 (2013) 13784-13789.

[27] X. Wang, H. Zhu, G.W. Greene, J. Li, N. Iranipour, C. Garnier, J. Fang, M. Armand, M. Forsyth, J. Pringle, P. C. Howlett, Enhancement of ion dynamics in organic ionic plastic crystal/PVDF composite electrolytes prepared by co-electrospinning, *J. Mater. Chem. A* 4 (2016) 9873-9880.

[28] Rao J., Vijayaraghavan R., Chen F., Zhu J., Howlett P., MacFarlane D. R., M. Forsyth, Protic organic ionic plastic crystals based on a difunctional cation and the triflate anion: a new solid-state proton conductor, *Chemical Communications* 52 (2016) 14097-14100.

FIGURES

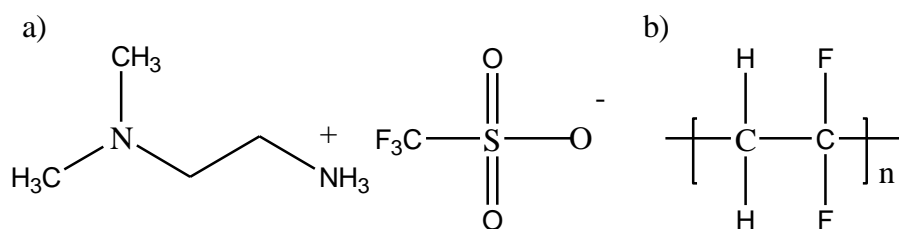


Figure 1. Chemical structures of: a) *N,N*-dimethylethylene diammonium triflate [DMEDAH][TFO]; b) poly(vinylidene fluoride) (PVDF).

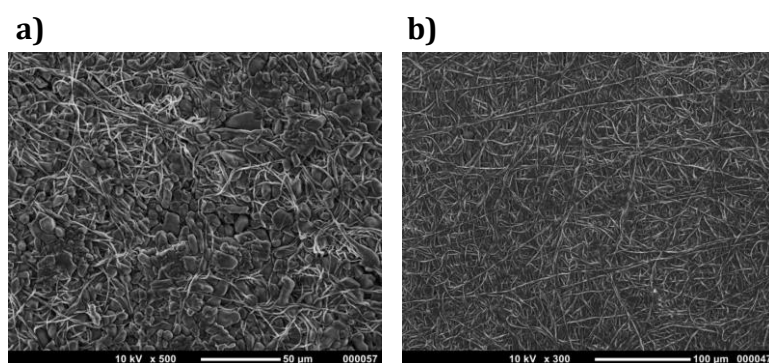


Figure 2. Pure [DMEDAH][TFO]/PVDF (90/10 wt%) membrane: a) SEM image front side; b) SEM image back side.

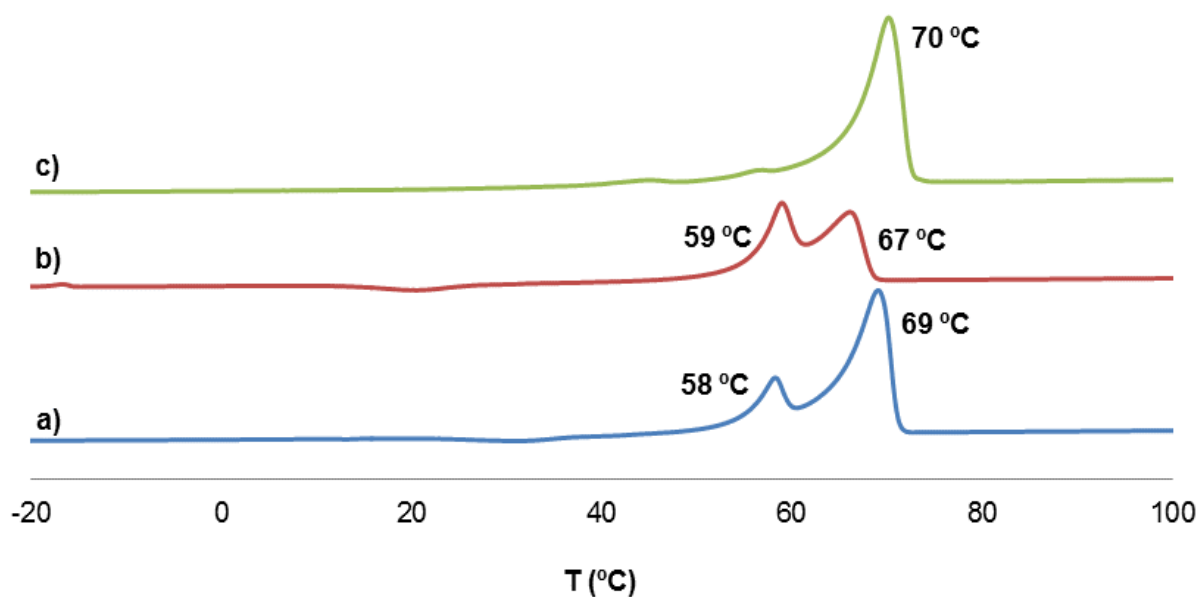


Figure 3. DSC thermal traces of (a) pure [DMEDAH][TFO], (b) 5 mol% acid-doped [DMEDAH][TFO] (c) and 5 mol% base-doped [DMEDAH][TFO].

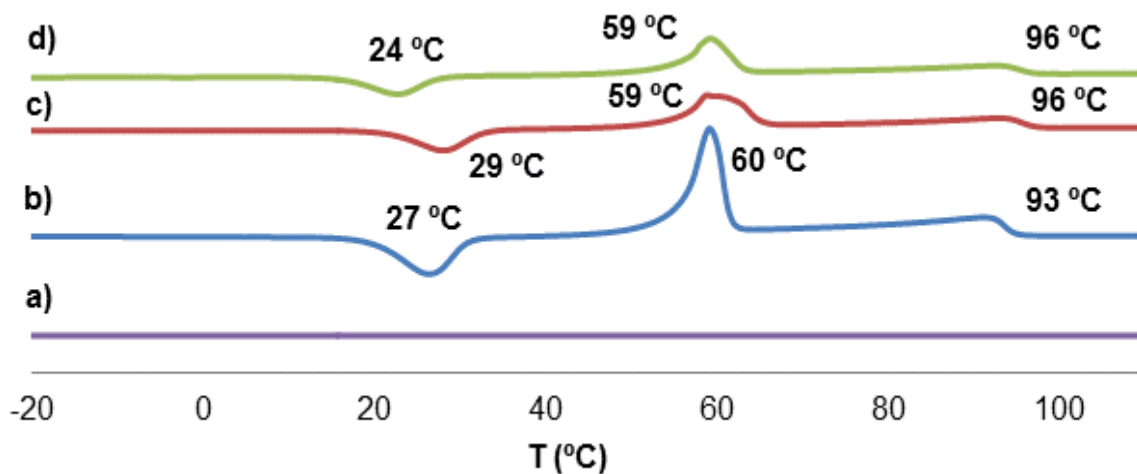


Figure 4. DSC thermal traces of (a) PVDF nanofibers, (b) PVDF/[DMEDAH][TFO], (c) PVDF/5 mol% acid-doped [DMEDAH][TFO] and (d) PVDF/5 mol% base-doped [DMEDAH][TFO] composite membranes.

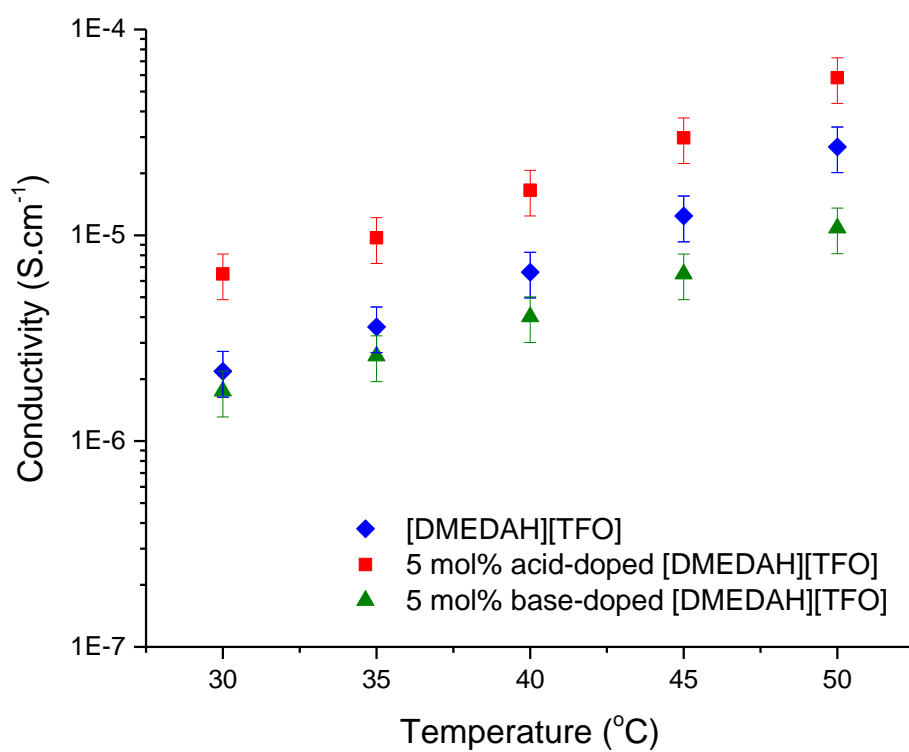


Figure 5. Ionic conductivity of pure and doped plastic crystals. [DMEDAH][TFO] (◆), 5 mol% acid-doped [DMEDAH][TFO] (■) and 5 mol% base-doped [DMEDAH][TFO] (▲).

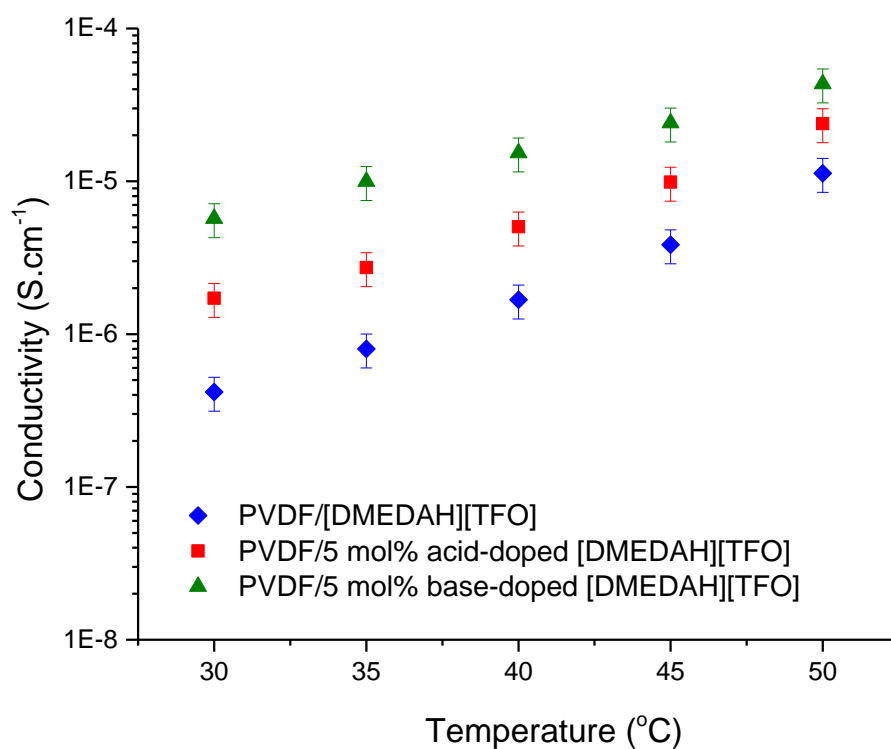


Figure 6. Ionic conductivity of PVDF/plastic crystal composite membranes. PVDF/[DMEDAH][TFO] (◆), PVDF/5 mol% acid-doped [DMEDAH][TFO] (■) and PVDF/5 mol% base-doped [DMEDAH][TFO] composite membranes (▲).

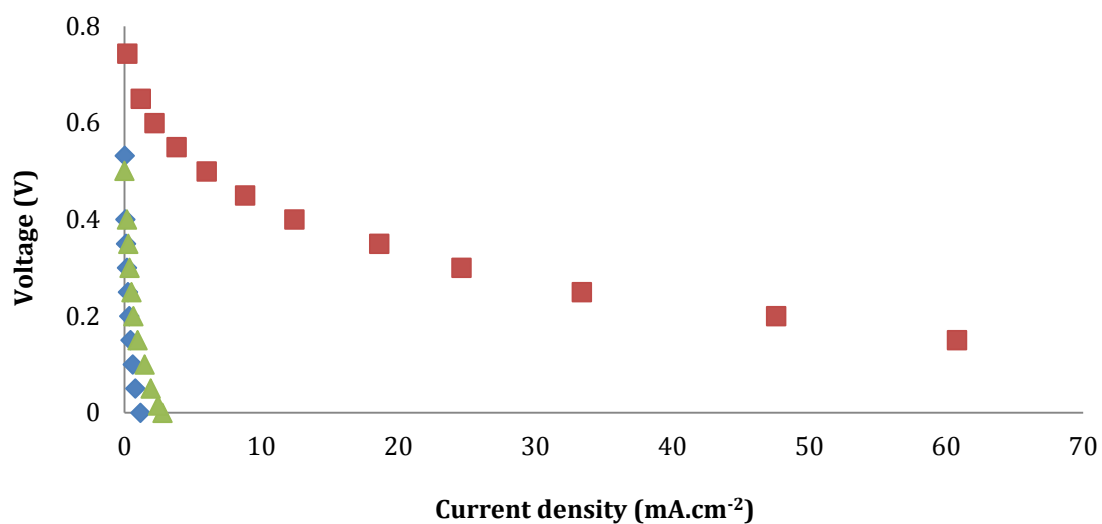


Figure 7. Polarization curves obtained with PVDF-based membranes. PVDF/[DMEDAH][TFO] (◆), PVDF/5 mol% acid-doped [DMEDAH][TFO] (■) and PVDF/5 mol% base-doped [DMEDAH][TFO] composite membranes (▲).

Table 1. Conductivity of the organic ionic plastic crystal (OIPC) [DMEDAH][TFO], the doped OIPC and the composites with PVDF.

T (°C)	log (conductivity/S cm ⁻¹) +/-0.1					
	OIPC	OIPC + 5 mol% acid	OIPC + 5 mol% base	PVDF/OIPC	PVDF / OIPC + 5 mol% acid	PVDF / OIPC + 5 mol% base
30	-5.7	-5.2	-5.2	-6.4	-5.8	-5.2
35	-5.4	-5.0	-5.0	-6.1	-5.6	-5.0
40	-5.2	-4.8	-4.8	-5.8	-5.3	-4.8
45	-4.9	-4.5	-4.5	-5.4	-5.0	-4.6
50	-4.6	-4.2	-4.2	-4.9	-4.6	-4.4